Annual and semiannual variations of the location and intensity of large-scale field-aligned currents

S. Ohtani
Johns Hopkins University Applied Physics Laboratory, Laurel, Maryland, USA

G. Ueno and T. Higuchi
Research Organization of Information and Systems, Institute of Statistical Mathematics, Tokyo, Japan

H. Kawano
Department of Earth and Planetary Sciences, Kyushu University, Fukuoka, Japan

Received 16 June 2004; revised 2 September 2004; accepted 13 October 2004; published 22 January 2005.

[1] The present study examines seasonal variations of large-scale field-aligned current (FAC) systems in terms of the dipole tilt and clock angles. Magnetic field measurements from the DMSP F7 and F12-F15 satellites are used. This data set consists of a total of ~185,000 auroral oval crossings, out of which ~121,000 crossings were selected for the present analysis. Focus is placed on the latitude at the demarcation between the region 2 (R2) and region 1 (R1) currents and the intensities of these currents. It is found that the dayside FAC moves poleward and equatorward in the summer and winter hemispheres, respectively, and the nightside FAC has the opposite seasonal dependence. In the midday sector the peak-to-peak variation of the FAC latitude over the entire range of the dipole tilt is ~5°, whereas it is ~4° around midnight. In the flank sectors the average FAC latitude is higher around the solstices than around the equinoxes irrespective of hemisphere. The corresponding dependence on the dipole clock angle can actually be found for almost all local time sectors, although the peak-to-peak variation of the expected semiannual variation, 2° around noon and <1° in other local time sectors, is smaller than that of the annual variation except for the flank sectors. A comparison with a model magnetic field strongly suggests that the dipole tilt effect on the magnetospheric configuration is the primary cause of the annual variation, whereas the semiannual variation is inferred to reflect the fact that geomagnetic activity tends to be higher around the equinoxes. The average dayside FAC intensity is larger in the summer hemisphere than in the winter hemisphere, which can be explained in terms of the seasonal variation of the ionospheric conductivity. The dayside R1 current intensity depends more strongly on the dipole tilt than the dayside R2 current intensity, and it changes by a factor of 2–3 over the entire range of the dipole tilt angle. In contrast, the annual variation of the nightside FAC intensity is more complicated, and the nightside R2 current seems to be more intense in the winter hemisphere than in the summer hemisphere. The dependence of the FAC intensity on the dipole clock angle is less significant especially for the R1 system. Nevertheless, the result suggests that the FAC tends to be more intense around the equinoxes, which is consistent with the semiannual variation of geomagnetic activity.

Citation: Ohtani, S., G. Ueno, T. Higuchi, and H. Kawano (2005), Annual and semiannual variations of the location and intensity of large-scale field-aligned currents, *J. Geophys. Res.*, *110*, A01216, doi:10.1029/2004JA010634.

1. Introduction

[2] The study of the field-aligned current (FAC) with satellite data has a long history, which started with the first detection of transverse magnetic disturbance in the auroral zone [*Zmuda et al.*, 1966] and subsequent interpretation/identification of such disturbances as satellite crossing of FACs [*Cummings and Dessler*, 1967; *Armstrong and Zmuda*, 1970]. The earlier statistical studies [*Zmuda and Armstrong*, 1974; *Sugiura*, 1975; *Iijima and Potemra*, 1976a] revealed a persistent polar distribution of FACs consisting of a pair of zonal current systems, which are now known as region 1 (R1) and region 2 (R2) systems. The R1 current flows downward and upward on the morning-side and eveningside, respectively, whereas the R2 current is located on the equatorward side of the R1 current and has the opposite polarity at a given local time. The R1 current is statistically most intense in the late morning

0148-0227/05/2004JA010634$09.00

and early afternoon sectors, but the nightside FAC is intensified significantly during substorms [*Iijima and Potemra*, 1978].

[3] In the midday sector, there is another FAC system [*Iijima and Potemra*, 1976b], which was initially named cusp current because of its location poleward of the R1 current [*Iijima and Potemra*, 1976b] and was later called by different names such as traditional cusp current [*Erlandson et al.*, 1988] and mantle current [*Bythrow et al.*, 1988] on the basis of comparison with collocated particle precipitation. In the present paper it will be referred to as R0 current since, in general, the midday FAC systems cannot be associated with any unique precipitation region [*Ohtani et al.*, 1995a, 1995b]. The distributions of the R0 and midday R1 currents, which are very often observed as a pair, strongly depend on the interplanetary magnetic field (IMF) B_Y component [e.g., *Iijima et al.*, 1978; *Erlandson et al.*, 1988].

[4] The seasonal variation of the FAC was one of the characteristics examined by earlier statistical studies [*Fujii et al.*, 1981; *Fujii and Iijima*, 1987]. Those studies found that dayside FACs tend to be more intense and to be located more poleward in summer than in winter. However, little attention has been paid to the issue since then. The recent revival of the issue [e.g., *Ohtani et al.*, 2000; *Christiansen et al.*, 2002; *Haraguchi et al.*, 2004; *Anderson and Korth*, 2004] can be attributed at least partly to the recognition of the active role of the ionosphere in the magnetosphere-ionosphere coupling based on recent observations. For example, on the nightside, auroral emission and intense electron precipitation tend to be enhanced in the winter hemisphere, where the ionosphere is dark [*Newell et al.*, 1996; *Liou et al.*, 2001; *Shue et al.*, 2001]. A similar seasonal dependence was also found for the occurrence of upward electron beams above the ionosphere [*Elphic et al.*, 2000; *Cattell et al.*, 2004]. It is also known that auroral dynamics are not necessarily conjugate between two hemispheres [*Sato et al.*, 1998; *Frank and Sigwarth*, 2003, and references therein]. Considering that the FAC is closely related to auroral acceleration, a better understanding of the seasonal variation of FACs should also provide useful insights about the seasonal dependence of auroral dynamics and conjugacy. The seasonal dependence of large-scale FACs was also addressed recently in attempts to model polar distributions of FACs under different external conditions [*Weimer*, 2001; *Papitashvili et al.*, 2002].

[5] Another interesting aspect of the seasonal variation of the FAC is the semiannual variation of geomagnetic activity, which has been reported for various geomagnetic indices [e.g., *Russell and McPherron*, 1973; *Berthelier*, 1976; *Cliver et al.*, 2000; *O'Brien and McPherron*, 2002]. It is intriguing to examine whether characteristics of the FAC reveal any similar semiannual variation.

[6] In the present study we examine seasonal variations of large-scale FAC systems using nearly 19 years worth of magnetic field data acquired from DMSP satellites [*Rich et al.*, 1985]. We previously developed an automatic procedure to identify spatial structures of FACs [*Higuchi and Ohtani*, 2000a, 2000b], and we applied it to each of ~185,000 auroral oval crossings, which likely provides the largest data set ever for studying statistical characteristics of FACs. In section 2 we describe the data set and this automatic procedure; a total of ~121,000 FAC crossings is selected for this study. We examine seasonal variations of the location (latitude) and intensity of the FAC in sections 3 and 4, respectively, along with their dependence on the dipole orientation. In section 5 we pay special attention to midday FACs. Results are discussed in section 6. Section 7 is a summary.

2. Data Set

[7] We use magnetometer data from the DMSP F7 (period of data used for this study: December 1983 to January 1988), F12 (September 1994 to November 2000), F13 (March 1995 to July 2000), F14 (December 1997 to September 2000), and F15 (December 1999 to September 2000) satellites. All DMSP satellites have Sun-synchronous orbits (F13 in an approximately dawn-dusk orientation and others in prenoon-premidnight orientations) at 835–850 km in altitude, and their orbital periods are ~100 min. The DMSP magnetic field experiments consist of triaxial fluxgate magnetometers with a range of ±65,535 nT and 1-bit resolution of 2 nT [*Rich et al.*, 1985]. The time resolution of data is 1 s.

[8] Figure 1 shows the spatial coverage of DMSP magnetometer data in the Northern (Figure 1a) and Southern (Figure 1b) hemispheres. In this study we use the altitude adjusted corrected geomagnetic (AACGM) coordinate system, which was previously known as the Polar Anglo-American Conjugate Experiment (PACE) system [*Baker and Wing*, 1989]; the AACGM latitude and longitude, which we calculate from the geographic coordinates of the satellite location, may be regarded as conventional corrected geomagnetic coordinates of the satellite magnetic foot point. Although the auroral zone is covered well in general, two cutoffs at high latitudes can be noticed especially in the Northern Hemisphere, one in the early afternoon and the other in the early morning sectors. The magnetic local time (MLT) coverage is better in the Southern Hemisphere owing to the larger offset of the magnetic pole from the geographic pole.

[9] *Higuchi and Ohtani* [2000a, 2000b] developed an automatic procedure to identify a structure of large-scale FACs along a satellite orbit, and we applied it to the DMSP data set. This procedure is based on the concept of the first-order B spline fit with variable node positions, which may be envisioned as fitting line segments to a line plot. The fitting is applied to the maximum variance component of horizontal magnetic variations. If the distribution of large-scale FACs can be approximated as an infinite sheet, each line segment corresponds to the crossing of a FAC sheet. The number of node points, which determines the number of FAC sheets, is one of the fitting parameters and is optimized for each oval crossing so that the Akaike information criterion is minimized. This procedure is basically the automation of the way we visually examine a plot of satellite magnetic field data.

[10] The goodness of the fitting can be evaluated for each event on the basis of three parameters. One is α, the square root of the maximum to minimum ratio of two eigenvalues of the maximum variance analysis of two horizontal components. This parameter measures how well the spatial structure of FACs can be locally approximated by an

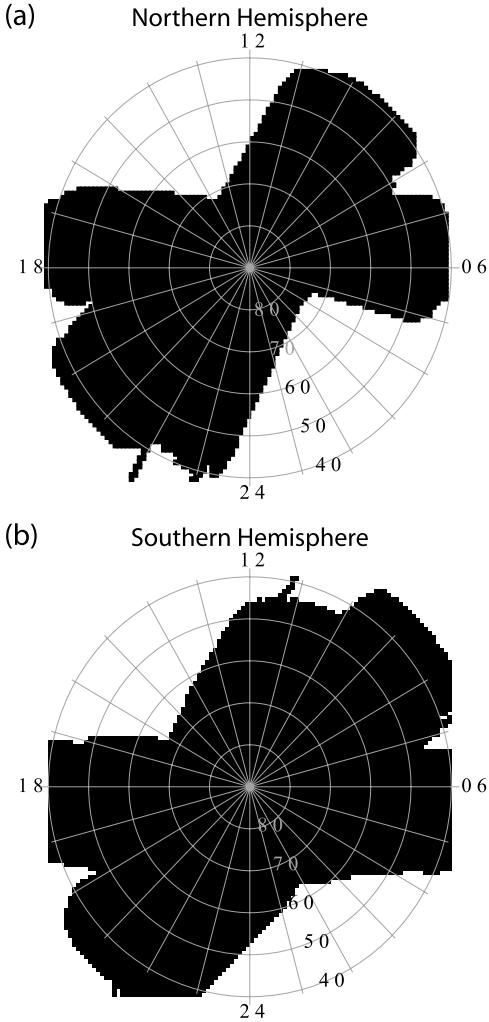

Figure 1. Spatial coverage of DMSP F7 and F12–F15 orbits in altitude adjusted corrected geomagnetic coordinates in the (a) Northern and (b) Southern Hemispheres.

extending sheet. The second parameter, Φ_Z, is the angle between the maximum variance orientation and the satellite cross-track direction. Φ_Z is 0° if the satellite crosses a FAC sheet (the maximum variance axis) vertically. The last parameter is R_{fit}, which is defined as the ratio (in percent) of the standard deviation of the difference between the optimum fit and the actual data to the magnitude of the magnetic change corresponding to the most intense FAC. Examples of the fitting to three-sheet structures with different values of R_{fit} are given by *Higuchi and Ohtani* [2000b, Figure 4]. R_{fit} becomes larger mostly because of structured magnetic field variations rather than because of less successful fit. In the present analysis we use only FAC crossings with $\alpha > 2$, $\Phi_Z < 45°$, and $R_{\text{fit}} < 12$. A total of ~121,000 FAC crossings was selected out of ~185,000 crossings for which we identified FAC structures.

[11] Figure 2 shows the number of FAC crossings in each 1-hour bin of MLT. Here the negative numbers are for crossings of downward FACs. The solid lines represent equatorwardmost FAC sheets (FAC-2), and the dashed and dotted lines represent the adjacent poleward (FAC-1) and the next poleward (FAC-0) sheets, respectively. In the present study we use the MLT and latitude of the polewardmost point of the FAC-2 sheet as representative coordinates of each FAC crossing, which we refer to as MLT_{12} and MLat_{12}, respectively. As will be addressed later in this section, they can be practically regarded as the coordinates of the R2/R1 demarcation.

[12] The distribution of FAC crossings has two broad peaks. One is in the dawn-to-prenoon sector, and the other is in the late afternoon-to-premidnight sector. We have far fewer crossings in the early morning and postnoon sectors; even in those sectors, however, the number of FAC crossings in each 1-hour bin exceeds 1100. The overall distribution of FAC crossings reflects the orbital characteristics of the DMSP satellites.

[13] In most MLT sectors, FAC-2 and FAC-1 are paired, which is inferred from the fact that the local time distributions of those currents are the mirror images of each other. The FAC-2 current tends to flow upward and downward in the morning and evening sectors, respectively, and at a given local time the preferred polarity of the FAC-1 current is opposite to that of the FAC-2 current. These characteristics confirm the well-known characteristics of the R2 and R1 systems [*Iijima and Potemra*, 1976a]. However, the preference of the FAC polarity is less clear in the midday and premidnight sectors, and the relative occurrence of FAC-0 currents is higher in those local time sectors. This complication presumably arises from the midday R0 current for the dayside and from substorm-associated FACs (or Harang discontinuity) for the nightside. In this paper we will simply refer to FAC-2, FAC-1, and FAC-0 as R2, R1, and R0 currents, respectively, and we will focus on events that have polarities consistent with the conventional distribution of those currents. However, the reader is advised to bear in mind that the identification of FACs in this study is based on their polarities. We will examine midday FACs with special attention in section 5.

3. Latitude

[14] In this section we examine the seasonal variation of the latitudes of large-scale FACs. Figure 3 plots the monthly median of the absolute value of MLat_{12}, $|\text{MLat}_{12}|$, in the Northern (solid) and Southern (shaded) hemispheres for each 2-hour bin of MLT_{12}. Error bars represent expected

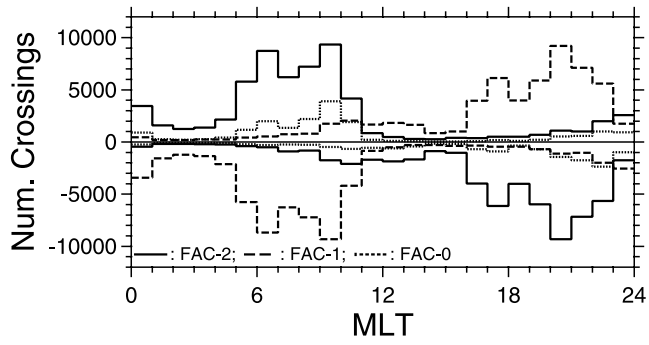

Figure 2. Numbers of crossings of the equatorwardmost (FAC-2), the secondmost equatorward (FAC-1), and the thirdmost equatorward (FAC-0) FACs for each 1-hour MLT bin. Negative numbers are for downward FACs.

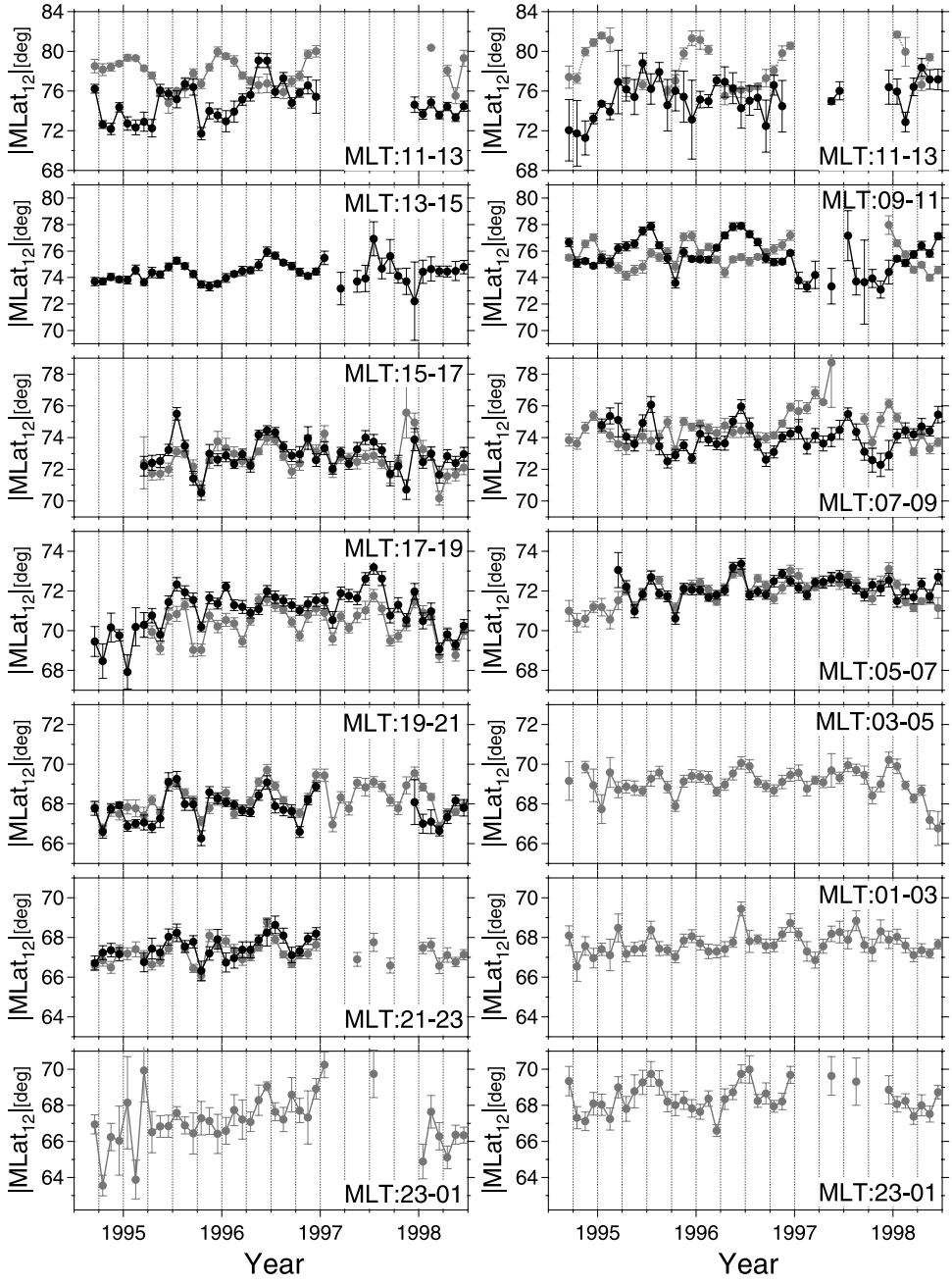

Figure 3. Monthly median values of $MLat_{12}$ in the Northern (solid) and Southern (shaded) hemispheres for each 2-hour bin of MLT_{12} for the 4-year interval of 1994.5–1998.5. The left (right) column is for eveningside (morningside) FAC structures with downward (upward) R2 currents.

errors for the averages. The same 4-year interval (1994.5–1998.5) is chosen for each panel. For some MLT sectors we have data only from a single hemisphere (for this specific interval but not necessarily for the entire interval of our data set) because of the restricted spatial coverage of orbits (Figure 1). The left (right) column in Figure 3 is for eveningside (morningside) FAC structures with downward (upward) R2 currents, and the MLT increases (decreases) downward from midday ($11 \leq MLT_{12} < 13$) to midnight ($23 \leq MLT_{12} < 1$). For the midday and midnight sectors, Figure 3 includes panels for both FAC structures. The vertical range is the same for two panels in the same row, but it varies from row to row, ranging from 16° (top row) to 8° (bottom four rows). For many FAC crossings in the midday sector, $MLat_{12}$ may actually represent the latitude at the R1/R0, rather than R2/R1, demarcation (section 5). However, as we will see below, the amplitude of the annual variation of $MLat_{12}$ is significantly larger than the typical latitudinal width of the dayside R1 current, $1° \sim 2°$ [*Iijima and Potemra*, 1976a]. Thus using $MLat_{12}$ as a representative latitude of the FAC location can be justified irrespective of local time.

[15] Let us start with the midday sector (panels labeled "MLT: 11–13" in Figure 3), where the monthly median of

$|MLat_{12}|$ reveals clear annual variations regardless of the polarity of the R2 current and is well anticorrelated between the Northern and Southern Hemispheres. The FAC system is located at higher and lower latitudes in summer and winter, respectively, with a peak-to-peak amplitude of several degrees. It is interesting to note that the baseline of $|MLat_{12}|$ is noticeably higher in the Southern Hemisphere than in the Northern Hemisphere, which might be related to different offsets of the dipole axis from geographic poles; such an offset, however, is less clear away from the midday sector.

[16] Similar annual variations can be found for the prenoon ($9 \leq MLT_{12} < 11$) and postnoon ($13 \leq MLT_{12} < 15$) sectors, but their peak-to-peak amplitudes are almost half that of the midday sector. Farther away from the noon meridian ($7 \leq MLT_{12} < 9$ and $15 \leq MLT_{12} < 17$), it is difficult to identify annual variations. In fact, $|MLat_{12}|$ tends to change in phase, rather than out of phase, between two hemispheres, and it seems that variations have a higher frequency. Such tendencies are clear in the dawn ($5 \leq MLT_{12} < 7$) and dusk ($17 \leq MLT_{12} < 19$) sectors. Irrespective of hemisphere, $|MLat_{12}|$ tends to be maximum in summer and winter and to be minimum in spring and fall. In other words, FAC systems tend to move poleward around the solstices and equatorward around the equinoxes. This semiannual variation can also be recognized for late evening and early morning sectors. In the midnight sector ($23 \leq MLT_{12} < 1$), however, annual variations, rather than semiannual variations, can be recognized again, especially for events with the morningside FAC structure. Note that $|MLat_{12}|$ in the Southern Hemisphere tends to peak in (southern) winter but not in (southern) summer as we found for the dayside sectors. In other words, the annual variations of dayside and nightside FAC latitudes seem to be 180° out of phase.

[17] It is reasonable to expect that those annual and semiannual variations of $MLat_{12}$ are related to the precession of the Earth's dipole axis, and the most straightforward test for this would be to examine $MLat_{12}$ in terms of dipole orientation. Here we consider the dipole orientation in terms of two angles. One is the conventional dipole tilt angle, ψ, which is the complement of the angle between the dipole axis and the Sun-Earth line (the GSE X axis), and the other is the clock angle in the Y-Z GSE plane, θ. In this study we measure θ from the GSE Z axis, rather than the GSE Y axis, for the convenience of the following analysis; we define θ positive toward the positive Y axis, but we will use only its absolute value $|\theta|$ in the following. The tilt angle ψ is positive and negative in northern summer and winter, respectively, whereas $|\theta|$ becomes larger around the equinoxes and smaller around the solstices. The value of ψ ranges from −35° to +35°, whereas the range of $|\theta|$ is from 0° to +35°. For analyzing the dependence on the dipole orientation we examine all selected FAC crossings not just those for the interval shown in Figure 3.

[18] In Figure 4 we examine the dependence of $|MLat_{12}|$ on ψ (Figures 4a–4d) and $|\theta|$ (Figures 4e–4h) for four representative 2-hour MLT sectors, that is, the dawn ($5 \leq MLT_{12} < 7$), midday ($11 \leq MLT_{12} < 13$), dusk ($17 \leq MLT_{12} < 19$), and midnight ($23 \leq MLT_{12} < 1$) sectors; for the midday and midnight sectors we selected events with the eveningside and morningside FAC structures, respectively. Each panel plots the median of $|MLat_{12}|$ against that of ψ ($|\theta|$) for each 5° (2.5°) wide bin along with the expected error of the average of $|MLat_{12}|$. The solid and shaded lines are for the Northern and Southern hemispheres, respectively. The vertical scales are different for different MLT sectors, but they are the same for the two panels of each sector. Generally speaking, in Figures 4a–4d, northern winter (southern summer) is to the left, and northern summer (southern winter) is to the right, whereas in Figures 4e–4h the solstices are to the left, and the equinoxes are to the right.

[19] For the midday sector (Figure 4b) the FAC tends to move poleward and equatorward as the magnetic pole moves toward and away from the Sun, respectively. The range of the latitudinal variation is 4°–5°, which one might think is significant considering that the average of $|MLat_{12}|$ is ~75°; that is, its colatitude is only 15° in the midday sector. For the duskside FAC (Figure 4c) a similar dependence can be found for the Northern Hemisphere, but no clear trend can be found for the Southern Hemisphere. In the dawn sector (Figure 4a) the tendency appears to be just the opposite of what we found for the midday sector, although the dependence on ψ is less systematic. That is, the FAC tends to move equatorward and poleward as the magnetic pole moves toward and away from the Sun, respectively. Such a countertrend can be found for the midnight sector with larger amplitudes (Figure 4d).

[20] In general, the dependence of $|MLat_{12}|$ on $|\theta|$, if at all, is weaker than that on ψ as can be seen from the fact that $|MLat_{12}|$ vary in narrower ranges. Nevertheless, we can still recognize that $|MLat_{12}|$ tends to decrease with increasing $|\theta|$ in the dusk sector (Figure 4g). For the dawn sector the tendency seems to be more systematic although the amplitude is much smaller (Figure 4e). In contrast, no clear tendency can be found for the midnight sector and for the midday Southern Hemisphere (Figures 4f and 4h).

[21] It appears that correlation between $|MLat_{12}|$ and ψ ($|\theta|$) varies significantly among local time sectors, suggesting that a more systematic analysis is required. We thus conducted a linear regression analysis for median values of $|MLat_{12}|$ in terms of ψ and $|\theta|$ for each 2-hour MLT sector; $|MLat_{12}|$ is expressed as $\alpha_\psi\psi + \beta_\psi$ and $\alpha_{|\theta|}|\theta| + \beta_{|\theta|}$. The coefficients, α_ψ and $\alpha_{|\theta|}$, are plotted in Figures 5a and 5c, whereas Figures 5b and 5d plot the corresponding correlation coefficients, CC_ψ ($CC_{|\theta|}$); the error bars for α_ψ and $\alpha_{|\theta|}$ are calculated on the basis of the averages of expected errors for the average values of $|MLat_{12}|$. The circles and squares represent FAC crossings in the Northern and Southern hemispheres, respectively, and FAC crossings are also classified into morningside (solid symbols) and eveningside (open symbols) latitudinal structures on the basis of the polarity of the R2 current. The coefficient (α_ψ or $\alpha_{|\theta|}$) is plotted only if the corresponding correlation coefficient is significant ($|CC| > 0.5$).

[22] On the dayside, α_ψ is positive in the Northern Hemisphere and is negative in the Southern Hemisphere; that is, the dayside FAC system moves poleward and equatorward in the summer and winter hemispheres, respectively. For $|\alpha_\psi| = 0.07$, the value for the northern midday sector, $|MLat_{12}|$ changes by 5° over the entire range of ψ. The amplitude of the variation decreases toward dawn as indicated by the decrease of $|\alpha_\psi|$, and the dependence of $|MLat_{12}|$ on ψ seems to be reversed around MLT = 6. Farther

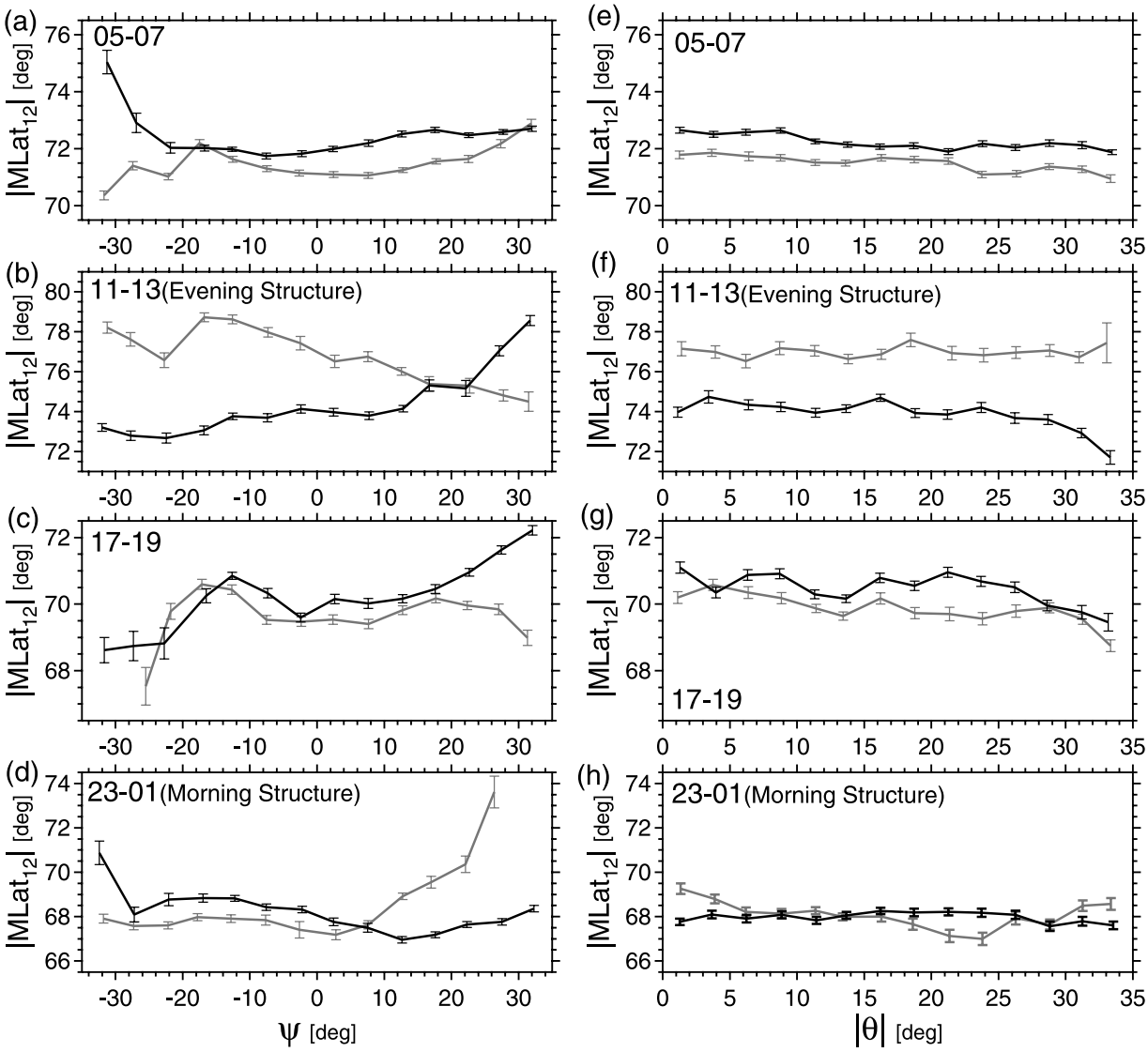

Figure 4. (a–d) $|MLat_{12}|$ versus ψ and (e–h) $|MLat_{12}|$ versus $|\theta|$ for four different MLT sectors (MLT = 5–7, 11–13, 17–19, and 23–1). The solid and shaded lines are for the Northern and Southern hemispheres, respectively. For the midday and midnight sectors we selected events with the eveningside and morningside FAC structures, respectively.

on the nightside, α_ψ is negative in the Northern Hemisphere and is positive in the Southern Hemisphere. In the dusk-to-midnight sector, in contrast, no significant correlation can be found between $|MLat_{12}|$ and ψ. It is possible that in that local time sector the dependence on the dipole tilt is masked by another factor that also controls the FAC latitude, for which geomagnetic (substorm) activity may be a good candidate.

[23] Correlation between $|MLat_{12}|$ and $|\theta|$ is equally high. The value of $\alpha_{|\theta|}$ is consistently negative (Figure 5c) irrespective of MLT or hemisphere; that is, the average latitude of FAC systems moves equatorward (poleward) when $|\theta|$ is large (small), therefore around the equinoxes (the solstices). The absolute value of $\alpha_{|\theta|}$ seems to be larger in the midday sector than in other sectors. Although error bars are larger there, all three points with reasonable correlation have large negative values. Otherwise, $\alpha_{|\theta|}$ does not show any clear local time dependence. For $\alpha_{|\theta|} = -0.06$ (for the midday sector) and -0.025 (for other sectors) the ranges of the variation of $|MLat_{12}|$ over the entire range of $|\theta|$ are 2° and 0.8°, respectively, which are significantly smaller than the corresponding value for ψ except for the flank sectors. This explains why we could most easily recognize the semiannual variation of $|MLat_{12}|$ for the dawn and dusk sectors in Figure 3. In other local time sectors the semiannual variation is presumably masked by the annual variation because of its smaller amplitude.

4. Intensity

[24] In this section we examine the intensities of FACs. Figures 6 and 7 plot the intensities of R2 and R1 currents, respectively, in the same format as Figure 3. The current intensity is positive and negative for upward and downward FACs, respectively, and the vertical axis is inverted for downward currents. Compared to $MLat_{12}$ (Figure 3), it is generally difficult to find seasonal variations. Exceptions

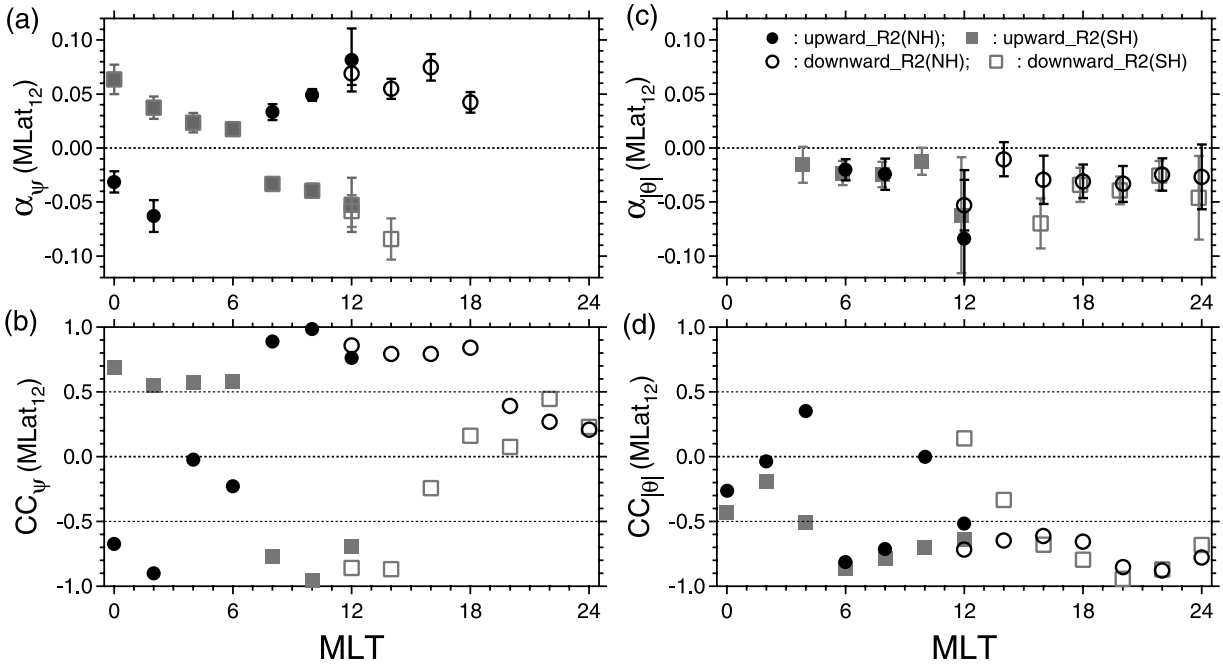

Figure 5. Results of the linear regression analysis of $|MLat_{12}|$ in terms of (a and b) ψ and (c and d) $|\theta|$ for each 2-hour MLT sector. Figures 5a and 5c plot the coefficients, α_ψ and $\alpha_{|\theta|}$, respectively, of the fitted linear functions, $\alpha_\psi\psi + \beta_\psi$ and $\alpha_{|\theta|}|\theta| + \beta_{|\theta|}$, and Figures 5b and 5d plot the corresponding correlation coefficients, CC_ψ and $CC_{|\theta|}$, respectively. The circles and squares represent FAC crossings in the Northern and Southern hemispheres, respectively, and the solid and open symbols are for the morningside and eveningside latitudinal structures, respectively. Here $\alpha_{|\theta|}$ is plotted with a horizontal offset for visibility.

are upward R2 currents in three morning sectors (MLT = 5–7, 7–9, and 9–11) and downward R1 currents in the prenoon and midday sectors (MLT = 9–11 and 11–13), where the average FAC intensity is clearly larger in summer than in winter. Those downward R1 currents especially reveal clear out-of-phase changes between Northern and Southern Hemispheres, and the interhemispheric difference can be a few hundred nanoteslas around the solstices (Figure 7). For the afternoon sector, however, we cannot identify any systematic annual variation of upward R1 currents. In general, the semiannual variation of the FAC intensity, whether it is the R2 or R1 current, is far more difficult to identify than that of the FAC latitude. The most likely, and possibly the only, candidate is the downward R2 current at 15 < MLT < 17.

[25] Next let us examine how the intensities of R2 and R1 currents depend on ψ and $|\theta|$ for each local sector. We fit linear functions $|I(Ri)| = \alpha_\psi(Ri)\psi + \beta_\psi(Ri)$ and $|I(Ri)| = \alpha_{|\theta|}(Ri)|\theta| + \beta_{|\theta|}(Ri)$ (I is FAC intensity, i is 1 and 2 for the R1 and R2 currents, respectively, and α_ψ and $\alpha_{|\theta|}$ are in units of mA m^{-1} deg^{-1}) to the median values as we did for $|MLat_{12}|$. Note that we consider the absolute value of the FAC intensity disregarding the FAC polarity. The results for the R2 and R1 currents are shown in Figures 8 and 9, respectively, which plot the coefficients, α_ψ and $\alpha_{|\theta|}$, and the corresponding correlation coefficients against MLT in the same format as Figure 5.

[26] One may find it intriguing that correlation is generally high in many local time sectors, except between $|I(R1)|$ and $|\theta|$, despite the difficulty in identifying annual and semiannual variations in the plots of monthly averages. The ψ dependence of R2 and R1 in dayside sectors, especially the late morning-to-noon sector, is very solid (correlation coefficients are close to 1 or −1). The dayside FAC tends to be more intense in the summer hemisphere and weaker in the winter hemisphere as indicated by the positive and negative values of α_ψ in the Northern and Southern Hemispheres, respectively. Obviously, the R1 current is more sensitive to ψ than the R2 current as indicated by the larger values of α_ψ. For $|\alpha_\psi| = 1$ the FAC intensity changes by 70 mA m^{-1} over the entire range of ψ. Thus the peak-to-peak amplitude of the annual variation of the R1 intensity in the late morning-to-noon sector is estimated at 200–400 mA m^{-1} from the corresponding values of α_ψ, which is comparable to the average intensities. For the nightside FAC the correlation tends to be lower (Figures 8b and 9b), and the peak-to-peak variation is <100 mA m^{-1} for both R2 and R1 currents. It is interesting that for the nightside (19 < MLT < 3) R2 current the sign of α_ψ is systematically the opposite to that on the dayside; in other words, the R2 intensity tends to be larger in winter. However, we cannot find any similar tendency for the nightside R1 current.

[27] Regarding the dependence of the R2 current intensity on the dipole clock angle, the value of $\alpha_{|\theta|}$ is biased positively (Figure 8c), suggesting that the R2 current tends to be more intense around the equinoxes than around the solstices; this also seems to be the case for the R1 current intensity as for the MLT sectors with reasonable (>0.5) correlation (Figure 9c). The peak-to-peak variation of the current intensity is estimated at several tens of milliamps per meter at maximum, which is a small fraction of the average

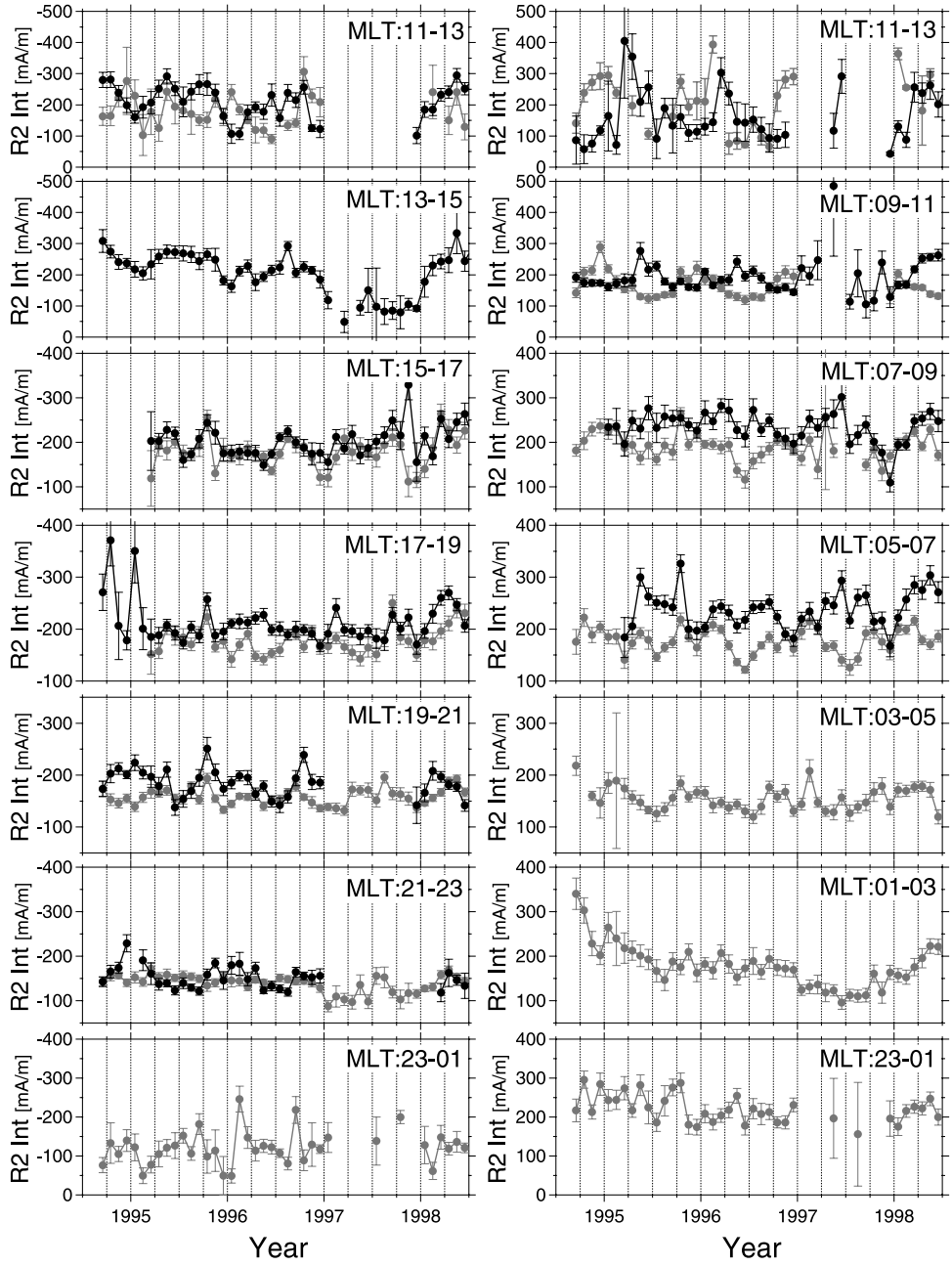

Figure 6. Monthly median values of the R2 current intensity in the Northern (solid) and Southern (shaded) hemispheres for each 2-hour bin of MLT_{12} for the 4-year interval of 1994.5–1998.5. The current intensity is positive and negative for upward and downward FACs, respectively, and the vertical axis is inverted for downward currents.

intensity; note that for $|\alpha_\theta| = 1$ the FAC intensity changes by 35 mA m^{-1} over the entire range of $|\theta|$, which is half of the corresponding value for ψ. This small amplitude explains why the semiannual variation could not be identified in Figures 6 and 7.

5. Midday FAC Systems

[28] We have been referring to the equatorwardmost and the secondmost equatorward FACs as R2 and R1 currents, respectively, following the convention. However, caution needs to be exercised for FACs in the midday sector, where the R2 current is often absent and two FAC sheets observed may be actually a pair of R1 and R0 currents [*Iijima and Potemra*, 1978]. Furthermore, because the demarcation between prenoonside and postnoonside pairs of R1 and R0 currents moves across the noon meridian depending on the IMF B_Y component [e.g., *Erlandson et al.*, 1988], it is difficult to identify midday FACs only from their polarities. For example, a pair consisting of an upward FAC on the equatorward side and a downward FAC adjacently poleward can be either a pair of prenoonside R2 and R1 currents or a pair of postnoonside R1 and R0 currents extending toward earlier local time across the noon meridian (when the IMF

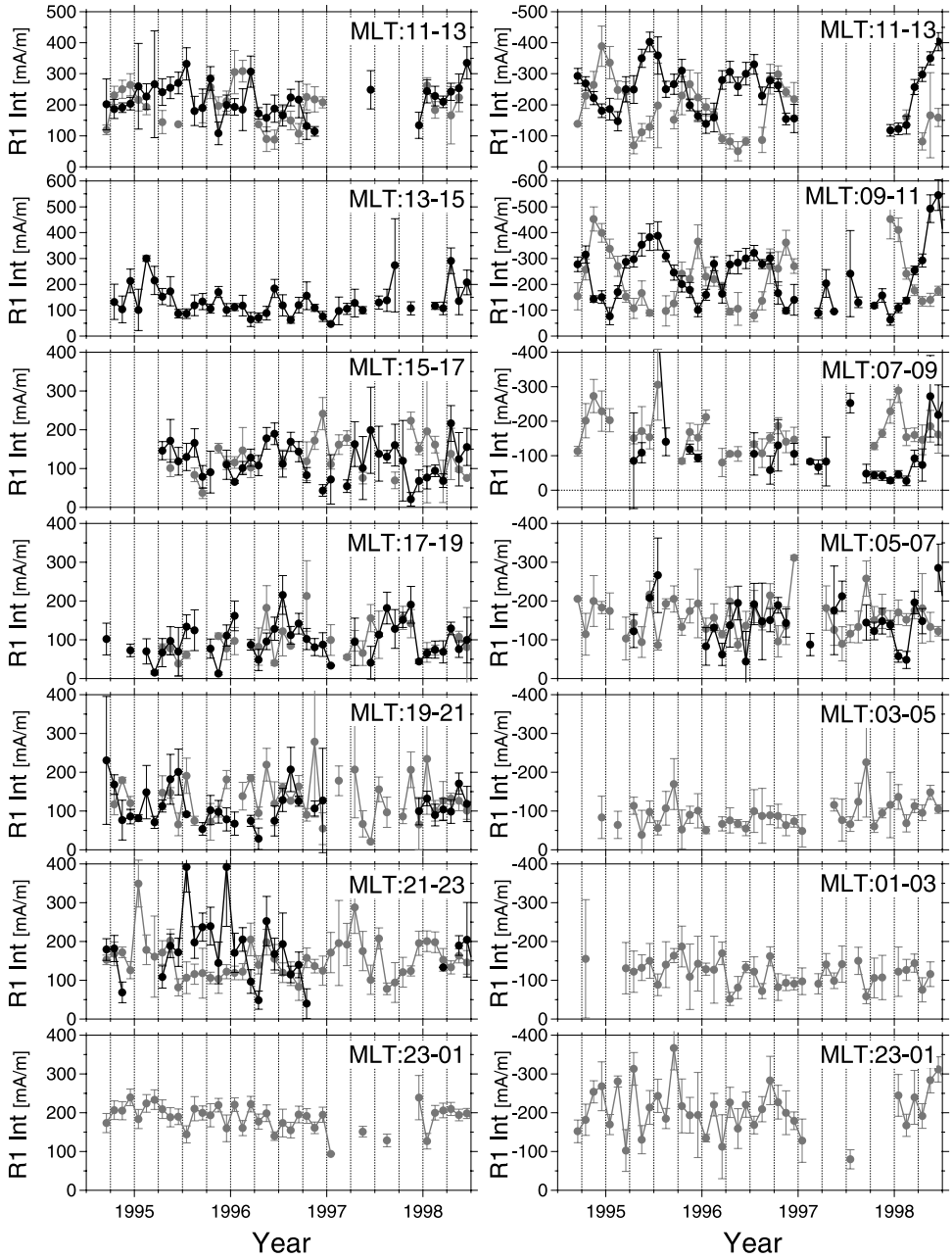

Figure 7. Same as Figure 6 but for the R1 current intensity.

B_Y component is negative and positive in the Northern and Southern Hemispheres, respectively). However, we occasionally observe three-sheet FAC structures. For such events we can confidently identify FACs as R2, R1, and R0 currents from equatorward, although one caveat is that the occurrence of the midday three-sheet structure itself may have some bias in terms of the IMF orientation or geomagnetic activity.

[29] In Figure 10 we focus on events with such three-sheet structures. From the top the number of events, $|MLat_{12}|$, and the intensities of R2, R1, and R0 currents are plotted against ψ. The left-hand and right-hand panels of Figure 10 are for the postnoonside (downward R2, upward R1, and downward R0 currents) and prenoonside (FACs with the opposite polarities) latitudinal structures, respectively. The dashed lines represent the results based on all events (as examined in sections 3 and 4) for comparison.

[30] The number of three-sheet events is a small fraction of the total number of events, and accordingly, error bars are larger for those events. $|MLat_{12}|$ tends to be smaller for three-sheet structures. This is reasonable because for some two-sheet events the demarcation between midday R1 and R0 currents is misidentified as $MLat_{12}$, which shifts the distribution of $|MLat_{12}|$ poleward. Nevertheless, the ψ dependence does not depend on the event sets very much, and for the postnoon structure the dashed lines (all events) almost trace the solid lines (three-sheet events). Figures 10c and 10h suggest that the actual intensity of R2 currents can be significantly smaller than what we estimated for equatorwardmost currents. This is also reasonable because the R2 system almost disappears in the midday sector. The

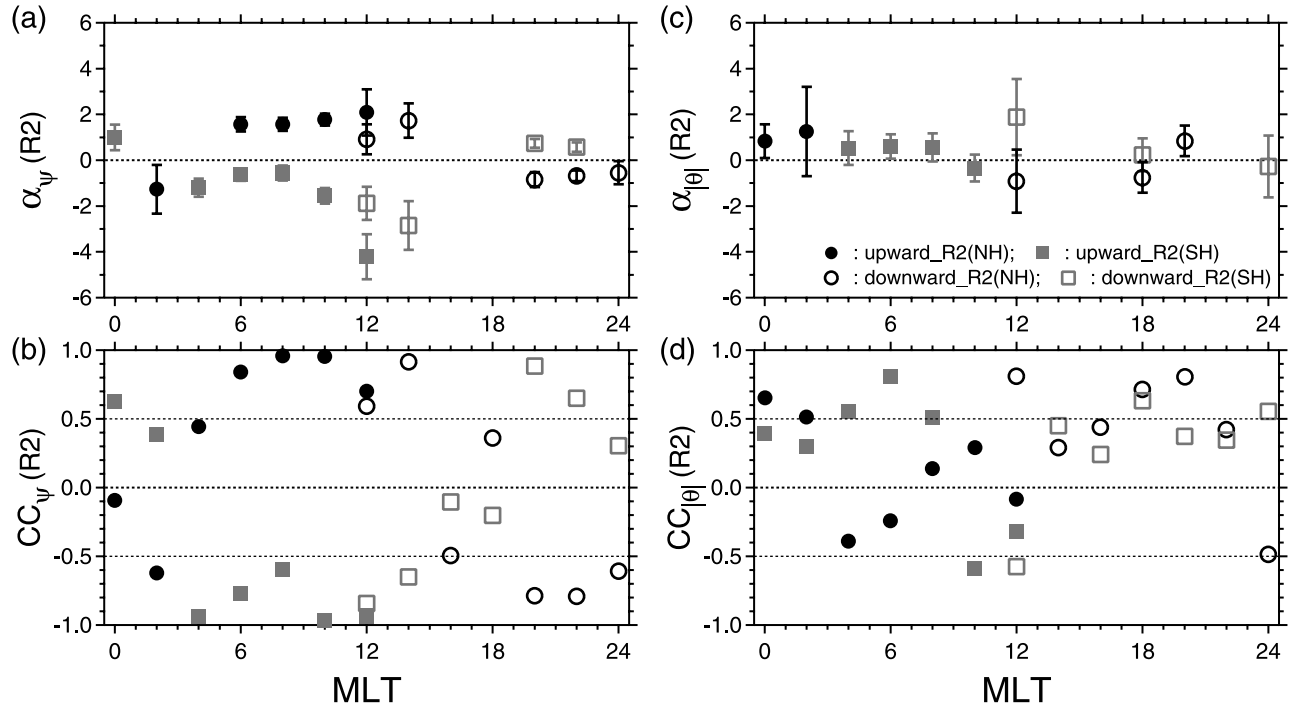

Figure 8. Same as Figure 5 but for the R2 current intensity.

tendency is just the opposite for the R1 current, although the relative difference is smaller (Figures 10d and 10i). We also emphasize that the R0 current tends to be more intense (weaker) in the summer (winter) hemisphere as do the other current systems (Figures 10e and 10j). In closing, although caution needs to be exercised for midday FACs, we infer that the results of our statistical study hold despite the uncertainty of the identification of midday FAC systems.

6. Discussion

[31] We found that dayside FACs move poleward and equatorward in summer and winter, respectively, and that

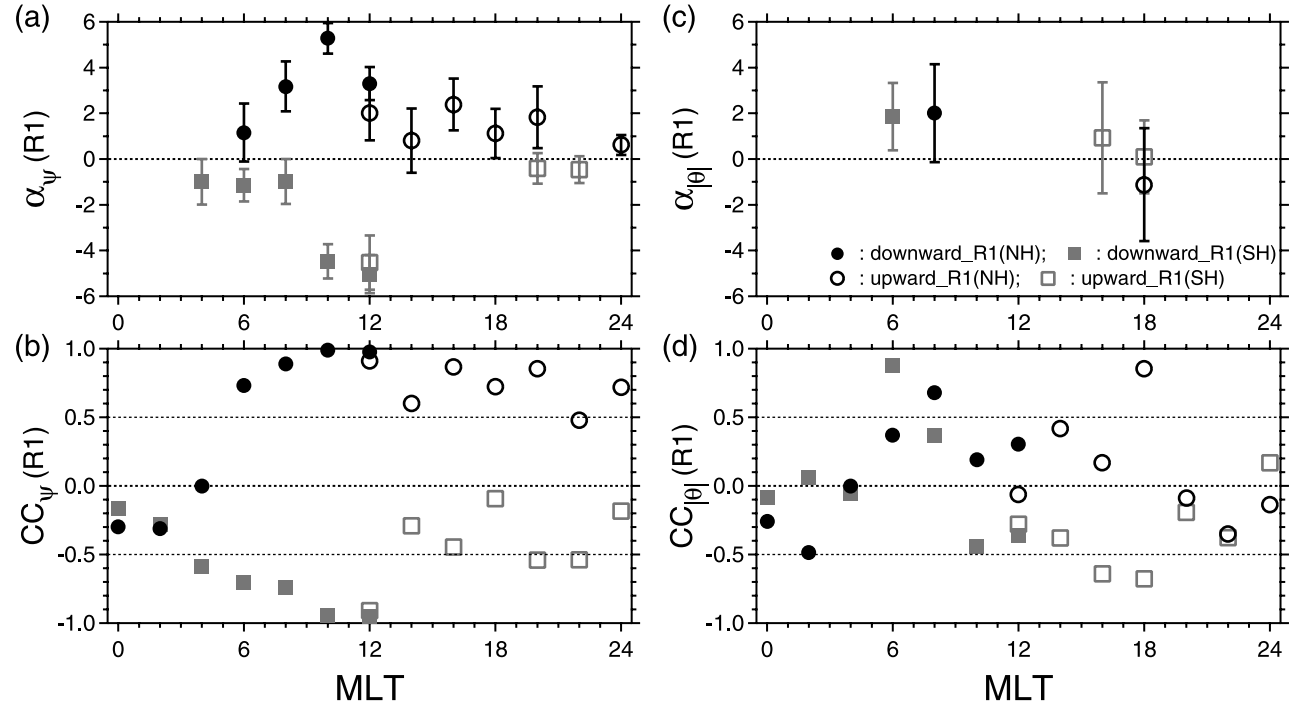

Figure 9. Same as Figure 5 but for the R1 current intensity.

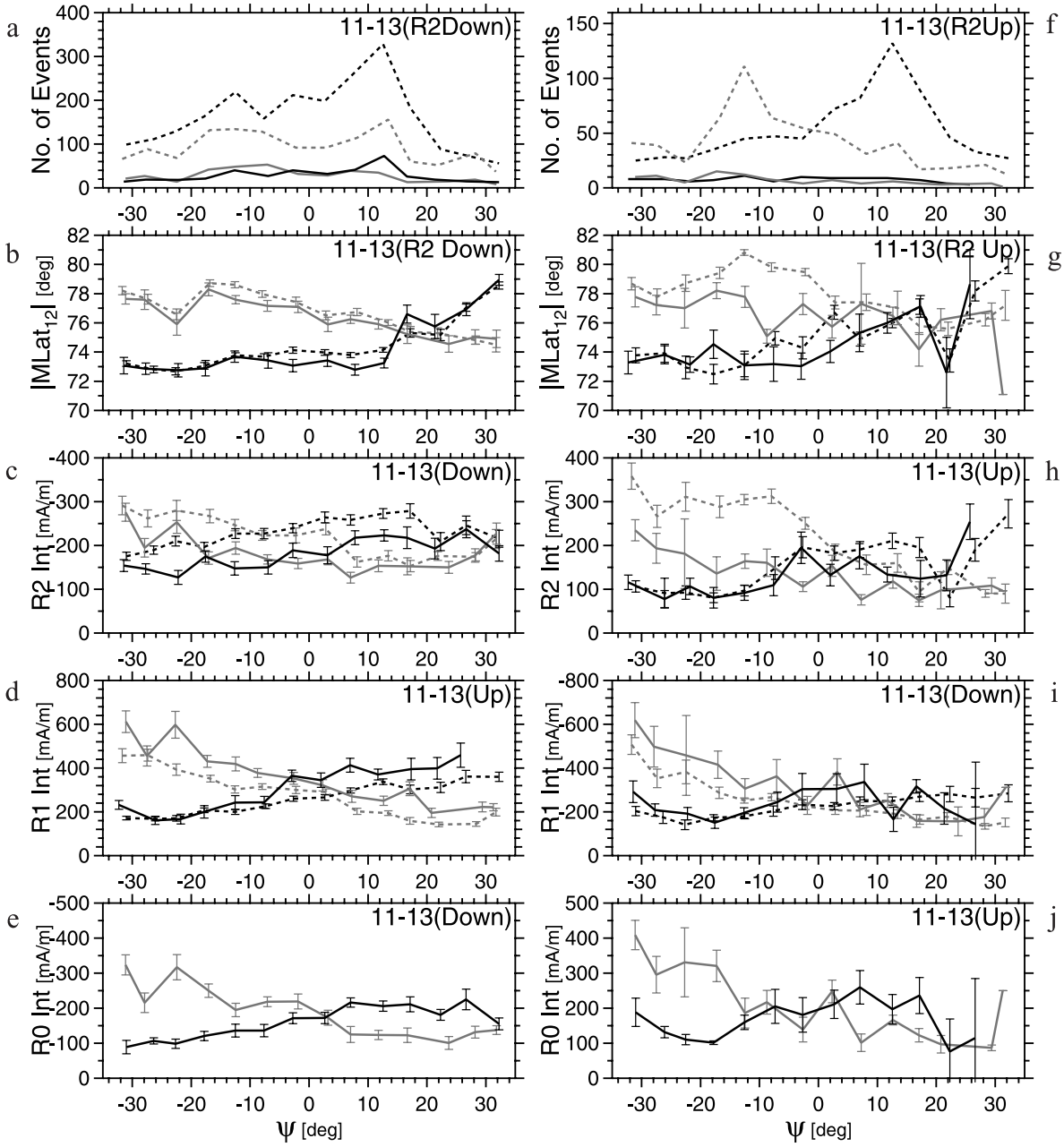

Figure 10. Dependence of the characteristics of (a–e) eveningside and (f–j) morningside three-FAC sheet events on the dipole tilt angle (ψ). Number of events (Figures 10a and 10f), latitude of the R2-R1 demarcation (Figures 10b and 10g), intensity of the R2 current (Figures 10c and 10h), intensity of the R1 current (Figures 10d and 10i), and intensity of the R0 current (Figures 10e and 10j) are plotted against ψ. The dashed lines in Figures 10a–10d and 10f–10i represent the results for the entire events.

the amplitude of this annual variation can be as large as 5° in latitude. *Fujii et al.* [1981] found that the average latitude of dayside FACs is higher in summer than in winter by 1°–3°. *Christiansen et al.* [2002] also found a similar tendency, although the difference between summer and winter hemispheres that they reported, 4°, is somewhat larger than the result of *Fujii et al.* [1981]. Thus, regarding the annual variation of the dayside FAC location, the present result is basically consistent with those previous results. *Newell and Meng* [1989] found that the average latitude of cusp particle precipitation is higher in summer and lower in winter, as we found for the dayside FAC, and their estimate of the peak-to-peak amplitude, 4°, also agrees with the present result. We therefore conclude that the dipole tilt affects the latitudes of dayside FACs and particle precipitation in a similar way.

[32] We also found that the nightside FAC moves equatorward and poleward in the summer and winter hemispheres, respectively. The amplitude of the latitudinal variation over the entire range of the dipole tilt angle is estimated at 4°. In contrast, *Christiansen et al.* [2002] reported that the average latitude of the quiet time (as measured by the northern polar cap magnetic activity index) nightside FAC is higher, rather than lower (as we found in

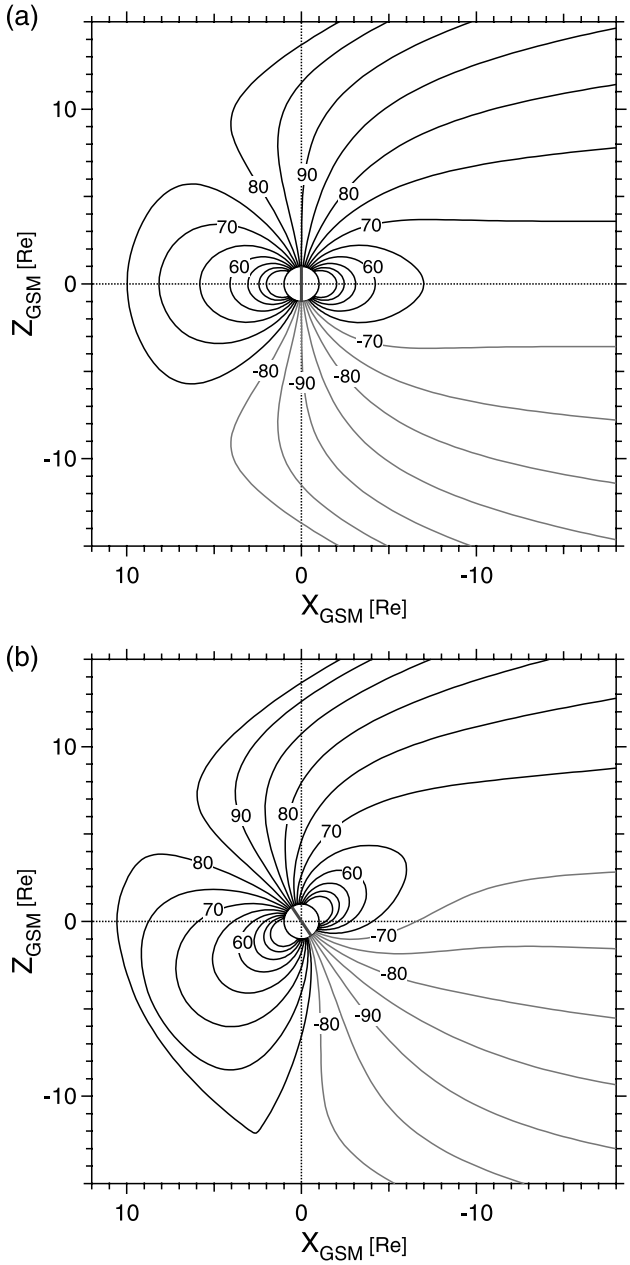

Figure 11. *X-Z* cross sections of the Tsyganenko 96 model (P_{dyn} = 3 nPa, *Dst* = 0 nT, IMF B_Y = 0 nT, and IMF B_Z = 0 nT) with the dipole approximation for the internal field for (a) the equinox and (b) the summer solstice.

this study), around the summer solstice than around the equinox; they estimated that the difference is 2° in latitude. The apparent discrepancy in the direction of the FAC motion between the two results might be attributed to the different definitions of the location of the FAC. Whereas we used the demarcation between R2 and R1 currents as a measure of the FAC latitude, *Christiansen et al.* [2002] used the average of the latitudinal range where the FAC density exceeds a certain threshold (0.1 μA m^{-2}). Thus it is likely that when the polar region is sunlit, the corresponding range extends poleward because of the higher ionospheric conductivity, which would move the average latitude poleward in summer overcompensating a geometrical effect that we will discuss next. In addition, the data set used by *Christiansen et al.* [2002] covers only single seasonal intervals for both the equinox and the solstice, and therefore, as they commented, their result might better be regarded as characterization of the time interval they examined.

[33] The most plausible cause of the annual variation of the FAC location is the interhemispheric asymmetry of the magnetospheric configuration between the winter and summer hemispheres. To test this idea, we examine a model magnetospheric configuration in terms of the dipole tilt. Here we use the Tsyganenko 96 (T96) model [*Tsyganenko*, 1996] along with the terrestrial dipole field. For the T96 model we assumed that P_{dyn} (solar wind dynamic pressure) = 3 nPa, *Dst* = 0 nT, IMF B_Y = 0 nT, and IMF B_Z = 0 nT. Figures 11a and 11b show the magnetic configurations in the *Z-X* GSM plane for the equinox ($\psi = 0°$) and the summer solstice ($\psi = 34°$), respectively. Field lines (solid) are traced from the Northern Hemisphere every 5° in geomagnetic latitude within 45° from the geomagnetic pole, and some selective field lines originating from the Southern Hemisphere are plotted by shaded lines. The inserted numbers denote geomagnetic latitudes of the foot points.

[34] The equinox configuration (Figure 11a) is symmetric with respect to the ecliptic plane, and the dayside cusps can be identified between the field lines originating at (−)75° and (−)80° in geomagnetic latitude. For the magnetic configuration for the summer solstice (Figure 11b) the ionospheric foot point of the northern cusp is located between 80° and 85° in geomagnetic latitude, whereas the foot point of the southern cusp is located equatorward of −80°. That is, in northern summer the northern cusp moves poleward. We also confirmed separately, as it is not clear in Figure 11, that the southern cusp moves equatorward at the same time. This seasonal dependence of the cusp latitude is consistent with the aforementioned result of *Newell and Meng* [1989], who also explained the annual variation in terms of the magnetospheric configuration.

[35] Figure 12 shows the effect of the dipole tilt on the magnetic configuration in a different way. Using the magnetic configuration shown in Figure 11b, we traced field

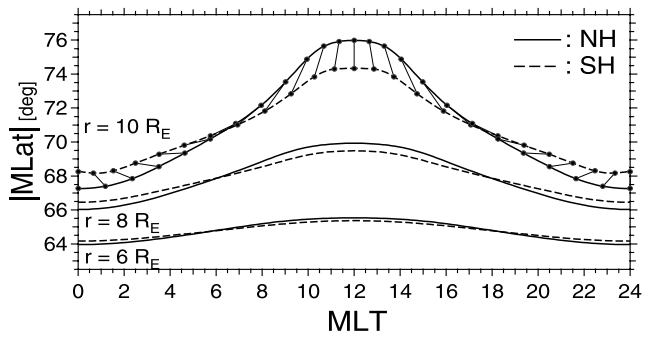

Figure 12. Northern and southern foot points of field lines traced from different geomagnetic equatorial distances (r = 6, 8, and 10 R_E) using the model magnetic field shown in Figure 11b. The conjugate points of the r = 10 R_E field lines are connected by superposed segments for every 1 hour in MLT at geomagnetic equator.

lines toward the northern and southern ionospheres from the magnetic equatorial plane at (r =) 6, 8, and 10 R_E from the Earth. We made the same calculation using the Tsyganenko 89 model for Kp = 1 [*Tsyganenko*, 1989, 1990] and found that the interhemispheric difference in the foot point latitude does not depend on the model very much. Figure 12 plots the absolute latitudes of northern (solid) and southern (dashed) foot points against MLT. The segments superposed to the r = 10 R_E foot points connect conjugate points for every 1 hour in MLT at the geomagnetic equator. For a given equatorial distance the latitude of the foot point is higher on the dayside because of the compression of the magnetic field by the solar wind, and it is lower on the nightside because of the antisunward stretching of the field line. The day-night asymmetry increases with the equatorial distance.

[36] On the dayside the foot point latitude is higher in the summer hemisphere than in the winter hemisphere, and the tendency is just the opposite on the nightside. The transition takes place around MLT = 6 and 18. For a given equatorial distance the interhemispheric difference, ΔMLat, is slightly larger on the dayside than on the nightside. For example, for r = 10 R_E it is ∼1.5° at noon and ∼1.0° at midnight. These numbers are smaller than our results (5° for the dayside and 4° for the nightside) by a factor of 3–4.

[37] Although this numerical experiment is meant to be a qualitative test (in fact, it is unrealistic that $MLat_{12}$ maps to the same radial distance on the equatorial plane), it is still interesting to consider reasons for this discrepancy. There are at least two possible explanations for this. First, ΔMLat increases with the equatorial distance. Therefore, if the demarcation between R2 and R1 currents is mapped to outside of r = 10 R_E, ΔMLat would be larger than what we estimated for r = 10 R_E. In fact, *Tsyganenko* [1990] found that the latitude of the last closed dayside field line can differ by several degrees between two hemispheres (see Figure 52 of their paper). Second, the response of the magnetospheric configuration to the IMF is not linear in terms of IMF B_Z, and therefore ΔMLat estimated for IMF B_Z = 0 nT does not represent its average. For example, as IMF B_Z decreases from 0 to −3 nT, ΔMLat increases from 1.5° to 2.3° at noon and from 1.0° to 1.9° at midnight, whereas it decreases only to 1.0° and 0.9° at noon and at midnight, respectively, as IMF B_Z increases from 0 to +3 nT. Thus it is highly likely that the average interhemispheric difference is weighed by cases of southward IMF B_Z and therefore should be larger than the present estimate for IMF B_Z = 0 nT. It is reasonable to conclude that the effect of the dipole tilt on the magnetospheric configuration is the main, if not the only, cause of the annual variation of the FAC latitude.

[38] From the viewpoint of the field line mapping we would like to make one additional comment. Both the field line modeling (Figure 12) and our analysis (Figure 5) reveal that the interhemispheric difference of the average FAC latitude is minimum in the flank sectors. This, however, does not mean that the northern and southern FACs are conjugate in those sectors. In Figure 12 the latitudinal difference between the foot points of the r = 8 and r = 10 R_E field lines is smaller in the Northern (summer) Hemisphere than in the Southern (winter) Hemisphere on the nightside and vice versa on the dayside. This indicates that as one traces a flux tube from the nightside equator toward the Earth, it is more pinched in the latitudinal direction in the Northern Hemisphere than in the Southern Hemisphere. Since the total flux must be conserved, this means that the flux tube becomes more elongated in the longitudinal direction in the Northern Hemisphere. In other words, a field line is mapped farther away from midnight to the northern ionosphere than to the southern ionosphere. In fact, for the r = 10 R_E field line the difference exceeds 1 hour in MLT at flanks; see the superposed segments, which connect the conjugate points.

[39] Nevertheless, the small annual variation of the FAC latitude in the flank sectors helped us recognize the semiannual variation of $|MLat_{12}|$ there (Figure 3). In other local time sectors the semiannual variation is masked by the annual variation because of its smaller amplitude (Figure 5). For the midday sector, $|MLat_{12}|$ changes by 2° over the entire range of $|\theta|$, whereas the corresponding amplitude for ψ is 5°. For other local time sectors the amplitude is <1°, although $|MLat_{12}|$ is well correlated with $|\theta|$ except for in the early morning sector.

[40] This semiannual variation is consistent with the well-known seasonal dependence of geomagnetic activity. The auroral oval expands when geomagnetic activity is high [*Kamide and Akasofu*, 1974; *Higuchi and Ohtani*, 2000a]. Thus the fact that the FAC latitude is lower in spring and fall and is higher in summer and winter suggests that geomagnetic activity tends to be higher around the equinoxes than around the solstices. Such a semiannual variation of geomagnetic activity has been studied for a long time [e.g., *Russell and McPherron*, 1973; *Berthelier*, 1976; *Cliver et al.*, 2000]. The Russell and McPherron (R-M) effect [*Russell and McPherron*, 1973] is well accepted as one of the causes of such semiannual variations. The effect is based on the idea that for the preferred IMF orientations in the ecliptic plane (the Parker spiral) the effective southward component of the IMF increases with the projection of the GSM Z axis to the GSE Y axis, which may be measured by θ.

[41] The fact that the intensity of R2 currents tends to increase with θ is consistent with this idea; Figure 8 shows that $\alpha_{|\theta|}$(R2) is positive for most MLT sectors with reasonable correlation. However, caution needs to be exercised because correlation is not significant for the R1 current, which we think somewhat puzzling since the R1 system is inferred to reflect more directly the solar wind-magnetosphere coupling except for substorm-related nightside currents. Note also that whether the R-M effect is the primary cause of the semiannual variation of geomagnetic activity is still controversial [*Cliver et al.*, 2000]. For the midday sector, however, it is well accepted that the dayside cusp moves equatorward as the IMF turns southward [*Burch*, 1973; *Newell et al.*, 1989], and therefore it may be less debatable to consider that the R-M effect is the primary cause of the semiannual variation of $MLat_{12}$.

[42] As for the FAC intensity the annual variation dominates the semiannual variation. The FAC tends to be more intense in the summer hemisphere than in the winter hemisphere. The amplitude of the annual variation is larger for the R1 system than for the R2 system, and it is also larger on the dayside than on the nightside; in fact, the dependence on the dipole tilt seems to be reversed for the nightside R2 current. The amplitude of the annual varia-

tion of the dayside R1 current intensity is of the same order as the average FAC intensity. In other words, the intensity of the dayside R1 current can differ by a factor of 2–3 between summer and winter; see also Figure 7. This is consistent with the result of the previous studies [*Fujii et al.*, 1981; *Fujii and Iijima*, 1987; *Christiansen et al.*, 2002; *Haraguchi et al.*, 2004]. A similar tendency can also be found in comparison of the polar maps of the FAC density between the winter and summer hemispheres [*Weimer*, 2001; *Papitashvili et al.*, 2002].

[43] The cause of the annual variation of the FAC intensity is most likely the annual variation of the ionospheric conductivity. The dayside ionospheric conductivity is determined mostly by the solar illumination, and therefore it strongly depends on the solar zenith angle [*Robinson and Vondrak*, 1984; *Rasmussen et al.*, 1988; *Moen and Brekke*, 1993], which is determined by the dipole tilt angle at given geomagnetic coordinates. The seasonal variation (or the dependence on the solar zenith angle at the ionospheric foot point) of the R1 intensity has been regarded as a feature suggestive of voltage generation at the R1 source [*Fujii and Iijima*, 1987; *Haraguchi et al.*, 2004]. The present study shows equally good correlation between the R2 intensity and ψ (Figure 8), though the result of *Haraguchi et al.* [2004] suggests otherwise. It is, however, questionable whether the generation of the R2 current is also a voltage source. It is perhaps more physical to address the nature of the FAC source on the basis of the current closure at the ionosphere rather than the ionospheric condition at the foot point of a specific FAC, which, however, is beyond the scope of this study.

7. Summary

[44] In this study we examined the seasonal variations of large-scale field-aligned current systems in terms of the tilt and clock angles of the Earth's dipole axis. The study is based on a FAC database created from DMSP magnetic field measurements, which consists of a total of ~185,000 auroral oval crossings, including ~121,000 crossings that were selected for the present analysis. Focus is placed on the average latitude of the R2/R1 demarcation and the intensity of FACs. The results can be summarized as follows:

[45] 1. The dayside FAC moves poleward and equatorward in the summer and winter hemispheres, respectively, and the tendency is just the opposite for the nightside FAC. In the midday sector the FAC latitude changes by 5° over the entire range of the dipole tilt angle, whereas the amplitude is estimated at 4° around midnight. The effect of the dipole tilt on the magnetospheric configuration is inferred to be the primary cause of this annual variation.

[46] 2. The FAC latitude also changes semiannually. The average FAC latitude tends to be higher around the solstices and to be lower around the equinoxes. Its peak-to-peak amplitude is estimated at 2° around noon and <1° in other local time sectors. This semiannual variation is consistent with the idea that geomagnetic activity tends to be higher around the equinoxes than around the solstices.

[47] 3. The average dayside FAC intensity is larger in the summer hemisphere than in the winter hemisphere by a factor of 2–3 for the R1 current, with a somewhat smaller factor for the R2 current. The seasonal variation of the ionospheric conductivity owing to the solar illumination is inferred to be the primary cause of those annual variations. In contrast, the annual variation of the nightside FAC intensity is less clear.

[48] 4. The semiannual variation of the FAC intensity is less clear especially for the R1 current. Nevertheless, the dependence on the dipole clock angle suggests that the FAC tends to be more intense around the equinoxes, which is inferred to reflect the semiannual variation of geomagnetic activity.

[49] **Acknowledgments.** Magnetometer data from the DMSP satellites were provided by F. J. Rich and the Air Force Research Laboratory. Routines for the Tsyganenko model and coordinated transformation were provided by N. Tsyganenko and T. P. O'Brien. Software for calculating AACGM (PACE) coordinates was provided by S. Wing and K. B. Baker. Work at APL was supported by NSF grant ATM-0101086. Work at the Institute of Statistical Mathematics was carried out in part under a Grant-in-Aid for Science Research (A) (14208025).

[50] Arthur Richmond thanks Vladimir Papitashvili and Nikolai Tsyganenko for their assistance in evaluating this paper.

References

Anderson, B. J., and H. Korth (2004), Simultaneous global-scale observations of field aligned currents in the Northern and Southern hemispheres, *Eos Trans. AGU*, *85*(17), Joint Assem. Suppl., Abstract SM24A-03.

Armstrong, J. C., and A. J. Zmuda (1970), Field-aligned current at 100 km in the auroral region measured by satellite, *J. Geophys. Res.*, *75*, 7122.

Baker, K. B., and S. Wing (1989), A new magnetic coordinate system for conjugate studies at high latitude, *J. Geophys. Res.*, *94*, 9139.

Berthelier, A. (1976), Influence of the polarity of the interplanetary magnetic field on the annual and the diurnal variations of magnetic activity, *J. Geophys. Res.*, *81*, 4546.

Burch, J. L. (1973), Rate of erosion of dayside magnetic flux based on a quantitative study of the dependence of polar cusp latitude on the interplanetary magnetic field, *Radio Sci.*, *8*, 955.

Bythrow, P. F., T. A. Potemra, R. E. Erlandson, L. J. Zanetti, and D. M. Klumpar (1988), Birkeland currents and charged particles in the high-latitude prenoon region: A new interpretation, *J. Geophys. Res.*, *93*, 9791.

Cattell, C. A., J. Dombeck, W. Yusof, C. Carlson, and J. McFadden (2004), FAST observations of the solar illumination dependence of upflowing electron beams in the auroral zone, *J. Geophys. Res.*, *109*, A02209, doi:10.1029/2003JA010075.

Christiansen, F., V. O. Papitashvili, and T. Neubert (2002), Seasonal variations of high-latitude field-aligned currents inferred from Orsted and MAGSAT observations, *J. Geophys. Res.*, *107*(A2), 1029, doi:10.1029/2001JA900104.

Cliver, E. W., Y. Kamide, and A. G. Ling (2000), Mountains versus valleys: Semiannual variation of geomagnetic activity, *J. Geophys. Res.*, *105*, 2413.

Cummings, W. D., and A. J. Dessler (1967), Field-aligned currents in the magnetosphere, *J. Geophys. Res.*, *72*, 1007.

Elphic, R. C., J. Bonnell, R. J. Strangeway, C. W. Carlson, M. Temerin, J. P. McFadden, R. E. Ergun, and W. Peria (2000), FAST observations of upward accelerated electron beams and the downward field-aligned current region, in *Magnetospheric Current Systems*, *Geophys. Monogr. Ser.*, vol. 118, edited by S. Ohtani et al., p. 173, AGU, Washington, D. C.

Erlandson, R. E., L. J. Zanetti, T. A. Potemra, P. F. Bythrow, and R. Lundin (1988), IMF B_y dependence of region 1 Birkeland currents near noon, *J. Geophys. Res.*, *93*, 9804.

Frank, L. A., and J. B. Sigwarth (2003), Simultaneous images of the northern and southern auroras from the Polar spacecraft: An auroral substorm, *J. Geophys. Res.*, *108*, 8015, doi:10.1029/2002JA009356.

Fujii, R., and T. Iijima (1987), Control of the ionospheric conductivities on large-scale Birkeland current intensities under geomagnetic quiet conditions, *J. Geophys. Res.*, *92*, 4505.

Fujii, R., T. A. Potemra, and M. Sugiura (1981), Seasonal dependence of large-scale Birkeland current intensities under geomagnetic quiet conditions, *Geophys. Res. Lett.*, *8*, 1103.

Haraguchi, K., H. Kawano, K. Yumoto, S. Ohtani, T. Higuchi, and G. Ueno (2004), Ionospheric conductivity dependence of dayside region-0, 1, and

2 field-aligned current systems: Statistical study with DMSP-F7, *Ann. Geophys.*, *22*, 2775.
Higuchi, T., and S. Ohtani (2000a), Automatic identification of large-scale field-aligned current structures and its application to night-side current systems, in *Magnetospheric Current Systems*, *Geophys. Monogr. Ser.*, vol. 118, edited by S. Ohtani et al., p. 389, AGU, Washington, D. C.
Higuchi, T., and S. Ohtani (2000b), Automatic identification of large-scale field-aligned current structures, *J. Geophys. Res.*, *105*, 25,305.
Iijima, T., and T. A. Potemra (1976a), The amplitude distribution of field-aligned currents at northern high latitudes observed by Triad, *J. Geophys. Res.*, *81*, 2165.
Iijima, T., and T. A. Potemra (1976b), Field-aligned currents in the dayside cusp observed by Triad, *J. Geophys. Res.*, *81*, 5971.
Iijima, T., and T. A. Potemra (1978), Large-scale characteristics of field-aligned currents associated with substorms, *J. Geophys. Res.*, *83*, 599.
Iijima, T., R. Fujii, T. A. Potemra, and N. A. Saflekos (1978), Field-aligned currents in the south polar cusp and their relationship to the interplanetary magnetic field, *J. Geophys. Res.*, *83*, 5595.
Kamide, Y., and S.-I. Akasofu (1974), Latitudinal cross section of the auroral electrojet and its relation to the interplanetary magnetic field polarity, *J. Geophys. Res.*, *79*, 3755.
Liou, K., P. T. Newell, and C.-I. Meng (2001), Seasonal effects on auroral particle acceleration and precipitation, *J. Geophys. Res.*, *106*, 5531.
Moen, J., and A. Brekke (1993), The solar flux influence on quiet time conductances in the auroral ionosphere, *Geophys. Res. Lett.*, *20*, 971.
Newell, P. T., and C.-I. Meng (1989), Dipole tilt angle effects on the latitude of the cusp and the cleft/LLBL, *J. Geophys. Res.*, *94*, 6949.
Newell, P. T., C.-I. Meng, D. G. Sibeck, and R. P. Lepping (1989), Some low-altitude cusp dependencies on the interplanetary magnetic field, *J. Geophys. Res.*, *94*, 8921.
Newell, P. T., C.-I. Meng, and K. M. Lyons (1996), Suppression of discrete aurorae by sunlight, *Nature*, *381*, 766.
O'Brien, T. P., and R. L. McPherron (2002), Seasonal and diurnal variation of *Dst* dynamics, *J. Geophys. Res.*, *107*, 1341, doi:10.1029/2002JA009435.
Ohtani, S., T. A. Potemra, P. T. Newell, L. J. Zanetti, T. Iijima, M. Watanabe, M. Yamauchi, R. D. Elphinstone, O. de la Beaujardière, and L. G. Blomberg (1995a), Simultaneous prenoon and postnoon observations of three field-aligned current systems from VIKING and DMSP-F7, *J. Geophys. Res.*, *100*, 119.
Ohtani, S., et al. (1995b), Four large-scale field-aligned current systems in the dayside high-latitude region, *J. Geophys. Res.*, *100*, 137.
Ohtani, S., T. Higuchi, T. Sotirelis, and P. T. Newell (2000), Disappearance of large-scale field-aligned current systems: Implications for the solar wind-magnetosphere coupling, in *Magnetospheric Current Systems*, *Geophys. Monogr. Ser.*, vol. 118, edited by S. Ohtani et al., p. 253, AGU, Washington, D. C.
Papitashvili, V. O., F. Christiansen, and T. Neubert (2002), A new model of field-aligned currents derived from high-precision satellite magnetic field data, *Geophys. Res. Lett.*, *29*, 1683, doi:10.1029/2001GL014207.
Rasmussen, C. E., R. W. Schunk, and V. B. Wickwar (1988), A photochemical equilibrium model for ionospheric conductivity, *J. Geophys. Res.*, *93*, 9831.
Rich, F. J., D. A. Hardy, and M. S. Gussenhoven (1985), Enhanced ionosphere-magnetosphere data from the DMSP satellites, *Eos Trans. AGU*, *66*, 513.
Robinson, R. M., and R. R. Vondrak (1984), Measurements of *E* region ionization and conductivity produced by solar illumination at high latitudes, *J. Geophys. Res.*, *89*, 3951.
Russell, C. T., and R. L. McPherron (1973), Semiannual variation of geomagnetic activity, *J. Geophys. Res.*, *78*, 92.
Sato, N., T. Nagaoka, K. Hashimoto, and T. Saemundsson (1998), Conjugacy of isolated auroral arcs and nonconjugate auroral breakups, *J. Geophys. Res.*, *103*, 11,641.
Shue, J.-H., P. T. Newell, K. Liou, and C.-I. Meng (2001), The quantitative relationship between auroral brightness and EUV Pedersen conductance, *J. Geophys. Res.*, *106*, 5883.
Sugiura, M. (1975), Identifications of the polar cap boundary and the auroral belt in the high-altitude magnetosphere: A model for field-aligned currents, *J. Geophys. Res.*, *80*, 2057.
Tsyganenko, N. A. (1989), A magnetospheric magnetic field model with the warped tail current sheet, *Planet. Space Sci.*, *37*, 5.
Tsyganenko, N. A. (1990), Quantitative models of the magnetospheric magnetic field: Methods and results, *Space Sci. Rev.*, *54*, 75.
Tsyganenko, N. A. (1996), Effects of the solar wind conditions on the global magnetospheric configuration as deduced from data-based field models, *Eur. Space Agency Spec. Publ.*, *ESA-SP 389*, 181.
Weimer, D. R. (2001), Maps of ionospheric field-aligned currents as a function of the interplanetary magnetic field derived from Dynamics Explorer 2 data, *J. Geophys. Res.*, *106*, 12,889.
Zmuda, A. J., and J. C. Armstrong (1974), The diurnal flow pattern of field-aligned currents, *J. Geophys. Res.*, *79*, 4611.
Zmuda, A. J., J. H. Martin, and F. T. Heuring (1966), Transverse magnetic disturbances at 1100 kilometers in the auroral region, *J. Geophys. Res.*, *71*, 5033.

T. Higuchi and G. Ueno, Research Organization of Information and Systems, Institute of Statistical Mathematics, Tokyo 106-8569, Japan.
H. Kawano, Department of Earth and Planetary Sciences, Kyushu University, Fukuoka 812-8581, Japan.
S. Ohtani, Johns Hopkins University Applied Physics Laboratory, Laurel, MD 20723, USA. (ohtani@jhuapl.edu)